1-1-2017

Electrochemical Oxidation of W(CO)4(LL): Generation, Characterization, and Reactivity of $[W(CO)4(LL)]^+$ (LL≤α-diimine ligands)

John P. Bullock
Bennington College, jbullock@bennington.edu

Chong Yong Lee
University of Wollongong, cylee@uow.edu.au

Brian Hagan
Bennington College

Humair Madhani
Bennington College

John Ulrich
Bennington College

Electrochemical Oxidation of W(CO)4(LL): Generation, Characterization, and Reactivity of $[W(CO)4(LL)]^{+}$ (LL≤α-diimine ligands)

Abstract

The electrochemistry of a series of W(CO)4(LL) complexes, where LL is an aromatic α-diimine ligand, was examined in coordinating and weakly coordinating media using several techniques. These compounds undergo metal-centred one-electron oxidations and the electrogenerated radical cations undergo a range of subsequent chemical steps, the nature of which depends on the substituents of the α-diimine ligand and the presence of coordinating species. In CH2Cl2/TBAPF6, where TBAPF6 is n-tetrabutylammonium hexaflurophosphate, the bulk oxidations are partially reversible at scan rates of 0.25Vs-1; the resulting tungsten(i) radicals react via disproportionation and loss of carbonyl, the rate constants for which were measured by double-potential step chronocoulometry. Large-amplitude a.c. voltammetry experiments suggest that the one-electron oxidized species are in equilibrium with the corresponding disproportionation products. Steric crowding of the metal centre prolongs the lifetime of the radical cations, allowing the infrared spectroelectrochemical characterization of two [W(CO)4(LL)]+ species. Electrogenerated [W(CO)4(LL)] + cations are highly susceptible to attack by potential ligands; oxidations performed in CH3CN/TBAPF6, for example, were chemically irreversible. Kinetic studies in weakly coordinating media show that near-stoichiometric amounts of added pyridine and acetonitrile are enough to greatly diminish the reversibility of the bulk oxidations; the dominant path of the coupled chemistry depends on the ligand strength, with substitution being the major reaction with added pyridine, whereas disproportionation is favoured by the presence of acetonitrile. A reaction scheme that provides an overall framework of the reactions followed by the radical cations is presented and discussed in the context of the previously observed chemistry of the molybdenum analogues.

Disciplines

Engineering | Physical Sciences and Mathematics

Publication Details

Bullock, J. P., Lee, C., Hagan, B., Madhani, H. & Ulrich, J. (2017). Electrochemical Oxidation of W(CO)4(LL): Generation, Characterization, and Reactivity of $[W(CO)4(LL)]^{+}$ (LL≤α-diimine ligands). Australian Journal of Chemistry: an international journal for chemical science, 70 (9), 1006-1015.

Electrochemical Oxidation of $W(CO)_4(LL)$: Generation, Characterization and Reactivity of $[W(CO)_4(LL)]^+$; (LL = α-diimine ligands)

John P. Bullock,*[a] Chong-Yong Lee, [b] Brian Hagan,[a] Humair Madhani, [a] John Ulrich [a]

Contribution from:

a. Division of Natural Science and Mathematics, Bennington College, Bennington, Vermont 05257, USA
b. Australian Research Council Centre of Excellence for Electromaterials Science, Intelligent Polymer Research Institute, AIIM, University of Wollongong, Innovation Campus, Wollongong, New South Wales, 2522, Australia

Abstract

The electrochemistry of a series of $W(CO)_4(LL)$ complexes, where LL is an aromatic diimine ligand, was examined in coordinating and weakly coordinating media using a range of techniques. Regardless of medium, these compounds undergo reversible one-electron oxidations, but the coupled chemistry is highly dependent on the presence of coordinating species. In $CH_2Cl_2/TBAPF_6$ the electrogenerated radical cation is stable enough on the cyclic voltammetry time-scale that the bulk electrode processes are partially reversible (i_c/i_a values are 0.6 - 0.9); the radicals react via disproportionation and loss of carbonyl, the rate constants for which were measured by double-potential step chronocoulometry. Large-amplitude ac voltammetry experiments revealed that the one-electron oxidized species are in rapid equilibrium with the corresponding disproportionation products. Steric crowding of the metal center was shown to prolong the lifetime of the radical cations, allowing for the infrared spectroelectrochemical characterization of two $[W(CO)_4(LL)]^+$ species. The presence of coordinating species dramatically diminishes the reversibility of the bulk oxidation; eg. oxidations performed in $CH_3CN/TBAPF_6$ were chemically irreversible. Kinetic studies in weakly coordinating media show that $[W(CO)_4(LL)]^+$ species are rapidly attacked by added pyridine and acetonitrile. After initially forming seven-coordinate, nineteen-electron species, these species undergo ligand substitution and disproportionation, the dominant paths for which depend on the nucleophile strength; disproportionation is the predominant reaction pathway with added acetonitrile while substitution was the major reaction with pyridine. A reaction pathway that provides an overall framework that describes the reaction processes the radical cations follow is presented and discussed in the context of previously observed reaction chemistry of the molybdenum analogs.

Introduction. Group 6 tetracarbonyl complexes of the type $M(CO)_4(LL)$, where LL is an aromatic α-diimine ligand, such as 2,2'-bipyridine (bpy), 1,10-phenanthroline (phen) or a substituted derivative thereof, comprise one of the most extensively studied classes of organometallic compounds.[1] Their relatively intense luminescence, arising from metal-to-ligand charge transfer excited states, makes them promising candidates for a variety of sensing and energy conversion schemes. They also have rich electrochemistry and more recently have been examined as electrocatalysts for the electroreduction of carbon dioxide.[2] Moreover, their structural simplicity make them useful compounds for examining the more general reactivity pathways for the ubiquitous $M(CO)_4$ moiety.

Because the excited states of these compounds formally involves an oxidized metal center and a reduced α-diimine ligand, electrochemical techniques have yielded significant insights into various aspects of their chemistry [3] Of particular interest have been the one-electron reduction processes exhibited by these and related compounds, many of which are chemically reversible. In contrast, the oxidative chemistry of such species has received far less attention. Several reports indicate that these compounds tend to undergo one-electron oxidations, the reversibility of which is highly dependent on the metal.[4,-6] In the case of tungsten, the rapid chemical reactions coupled to the electrode process make characterization of the electrogenerated species difficult, which has no doubt contributed to the paucity of studies of the seventeen-electron radical cations, $[W(CO)_4(LL)]^+$, $\mathbf{1}^+$. The chromium and molybdenum analogs, however, have been examined to a greater extent. The chromium compounds, in particular, show chemically reversible oxidations, and at least one such compound, $Cr(CO)_4$(tmp), where tmp = 3,4,7,8-tetramethyl-1,10-phenanthroline, has been spectroscopically characterized by several techniques.[6] Oxidation of $Mo(CO)_4$(bpy) was shown to be chemically reversible only in noncoordinating solvent/electrolytes.[7]

Several years ago, our laboratory investigated the chemistry of a variety of $Mo(CO)_4(LL)$ compounds to better characterize the chemical reactivity of the corresponding electrogenerated radical cations, $[Mo(CO)_4(LL)]^+$ using cyclic voltammetry and potential-step techniques. [8] In addition, by using a sterically hindering ligand, 2,9-dimethyl-1,10-phenanthroline, also known as neocuproine (ncp), we could stabilize the radical cation enough to characterize it via infrared spectroelectrochemistry. This paper describes our recent experiments that extend that work, delineating the chemistry of electrogenerated $\mathbf{1}^+$. As expected, these compounds share some similarities with their molybdenum analogs, but they also exhibit quite distinct electrochemical responses under some conditions. This work sheds light on the underlying reactivity patterns

shared by these compounds and provides a framework that makes possible a coherent view of their reaction pathways of this important class of Group 6 tetracarbonyl compounds.

Experimental.

Materials and Methods. Tungsten hexacarbonyl, $W(CO)_6$ (Strem), pyridine (Aldrich) and all ligands used in this study were used as received (GFS Chemicals, Aldrich); these included: 1,10-phenanthroline, **a** (phen), 2,2'-byridine, **b**, (bpy), the substituted phenanthroline ligands dimethylphenanthroline, **c** (dmp), 3,4,7,8-tetramethylphenanthroline, **d** (tmp), 4,7-diphenylphenanthroline, **e** (bph), 2,9-dimethyphenanthroline, **f** (ncp), 2,9-dimethyl-4,7-diphenylphenanthroline, **g** (bcp), 5-nitrophenanthroline, **h**, (nop), 5-chlorophenanthroline, **i** (clp), and the substituted bipyridyl ligand, 4,4'-dimethyl-2,2'-bipyridine, **j**, (dmb).Solvents used for electrochemical experiments, methylene chloride and acetonitrile (Aldrich), were HPLC grade. Tetrabutylammonium hexafluorophosphate, $TBAPF_6$, (Southwestern Analytical) was used as received. All solvent electrolyte solutions were dried over activated 4Å molecular sieves (Aldrich).

Syntheses. **1a-j** were prepared photolytically using a procedure adapted from the literature;[9] the synthesis of **1j** is presented below and typifies all such syntheses performed in this work,. $W(CO)_6$ (0.550 g, 1.56 mmol) was dissolved in 50 mL dry tetrahydrofuran (Pharmco) and degassed in a round bottom flask. The resulting solution was illuminated with a 100 W mercury arc lamp until nearly complete conversion to $W(CO)_5(THF)$ had been effected[10] as determined by infrared spectroscopy; this normally required three to four hours of constant illumination. To the resulting yellowish-green solutions was added a slight molar excess of dmp (0.347 g, 1.64 mmol) under constant stirring and nitrogen purge; this resulted in a rapid color change and eventual precipitation of the desired product. After thirty minutes, the precipitate was isolated and washed with additional THF; the crude product was purified by recrystallization from methylene chloride/hexanes. The product (0.516 g, 1.02 mmol, 65% yield) consisted of brick red crystals and its identity was confirmed by IR spectroscopy. Most of the compounds synthesized exhibited deep red luminescence as solids.

Instrumentation. Dc cyclic voltammetry and double potential-step chronocoulometry experiments were performed using a Bioanalytical Systems 50B electrochemical workstation using a 3 mm diameter glassy carbon working electrode and a Ag/Ag^+ pseudo-reference electrode. Oxidation potentials, $E°$, were measured using cobaltocenium hexafluorophosphate,

Cc^+, (Aldrich), as an internal standard. Analyte solutions were degassed and kept under nitrogen for all analyses. To facilitate comparisons with other reports, the $Cc^{+/0}$ redox couple was observed at -1.335 V vs the ferrocene/ferrocenium couple in CH_2Cl_2/$TBAPF_6$. Infrared spectroelectrochemical experiments were performed using a cell described previously[11] and a Thermoelectron Avatar 350 FTIR spectrometer; the BAS 50B workstation was used to control and monitor the electrolyses.

Large amplitude ac voltammetry was performed using a custom-built instrument as described elsewhere.[12] Data was analyzed using MECSIM software[13] and the following parameters were optimized via visual fit: uncompensated resistance, *R*, heterogeneous rate constant, *k°*, and relevant homogeneous rate constants; the transfer coefficient, α, was assumed to be 0.5 in all simulations. The diffusion coefficient for **1a** was calculated from chronocoulomeric data using the Cottrell equation.[14] Analyses of the data focused on the third through sixth harmonics, as these show little contribution from non-Faradaic current.

Kinetic Analysis. Determination of second-order disproportionation rate constants using chronocoulometric data were complicated by the presence of a simultaneous first order reaction as described in the text. To calculate the net rate of disproportionation, experimental data obtained at each analyte concentration were initially fit to a working curve for the theoretical response of a disproportionation mechanism;[15] using the corresponding best fit rate constants, k_{eff}, the overall reaction rate was estimated using a second order rate law. This overall rate of conversion of $\mathbf{1}^+$ was set equal to the sum of two separate process with rate constants k_{disp} and $k_{1st\text{-}order}$ (eq. 1). Linearization afforded values of $k_{1st\text{-}order}$ from the intercept and k_{disp} from the slope of the resulting plot (eq. 2).

$$rate \sim k_{eff}[[\mathrm{W(CO)_4(LL)}]^+]^2 \sim k_{disp}[[\mathrm{W(CO)_4(LL)}]^+]^2 + k_{1st-order}[\mathrm{W(CO)_4(LL)}]^+ \quad (1)$$

$$k_{eff}[\mathrm{W(CO)_4(LL)}]^+ \sim k_{disp}[[\mathrm{W(CO)_4(LL)}]^+] + k_{1st-order} \quad (2)$$

Results and Discussion.

Ten $W(CO)_4$(LL) compounds were examined in this study and are designated **1a-j** herein, with the letters corresponding to each α-diimine ligand as specified in the Materials section and in Table 1. For clarity, references in the text to either **1** or $\mathbf{1}^+$ should be assumed to be

representative of the entire class of compounds, whereas those to individual compounds, e.g., **1a**, are provided in the context of experimental data or to properties thought to be unique to a particular species.

Dc cyclic voltammetry studies. Cyclic voltammograms of **1a** and its molybdenum analog, $Mo(CO)_4(phen)$, in two different solvent/electrolyte media, are shown in Figure 1. As can be seen, the voltammetric responses of these compounds depend on the media in which the experiments are performed. In methylene chloride/$TBAPF_6$, a weakly coordinating medium, the tungsten and molybdenum compounds exhibit quasi-reversible one-electron oxidations (Figure 1, top), whereas in the more highly coordinating acetonitrile/$TBAPF_6$, the bulk oxidation is irreversible for complexes of both metals (Figure 1, bottom). This behavior is consistent with observations made previously in a thorough study of the electrochemical oxidation of $Mo(CO)_4(bpy)$ in a number of solvent/electrolyte systems[7] and also parallels that seen among the structurally analogous molybdenum and tungsten tetracarbonyl diazadiene[16] complexes.

The cyclic voltammogram of **1a** in CH_2Cl_2/$TBAPF_6$ shown in Figure 1 is typical for most of the complexes examined in this study measured under similar conditions; data for other compounds are summarized in Table 1. The bulk oxidations had i_c/i_a values ranging from 0.6 to slightly more than 0.9 at scan rates of 0.250 V s^{-1} and the oxidation potentials show expected trends based on the nature of the substituents on the α-diimine ligands. For example, $E°$ values of complexes are shifted negatively, relative to unsubstituted diimine ligands, when electron-donating methyl groups are present, such as with di- and tetra-methyl substituted phenanthroline, **1c** and **1d**, while those with electron-withdrawing groups, such as nitro- or choro-, **1h** and **1i**, are shifted positively.

Our results indicate that the tungsten and molybdenum $M(CO)_4(LL)$ compounds show similar oxidative electrochemistry in weakly coordinating media but with some notable differences. For example, the bulk oxidations of $M(CO)_4(LL)$ compounds for both metals are coupled to multiple coupled homogeneous processes. At a scan rate of 0.250 V s^{-1}, molybdenum compounds show three coupled reduction peaks in addition to that of the radical cation. In a previous study,[8] we assigned these peaks to reductions of a Mo^{2+} disproportionation product and two different Mo^{+} compounds, $[Mo(CO)_3(LL)D]^{+}$, formed via the loss of a CO ligand; here, D is the weakly coordinating PF_6^- supporting anion[17] in one case and adventitious water in the other. Tungsten compounds, in contrast, typically show only one coupled reduction peak, other than that due to the radical cation, at the same scan rate. We assign this peak to the reduction of a W^{2+} disproportionation product, $[W(CO)_4(LL)(D)]^{2+}$; potentials of the observed coupled reduction

peak maxima are included in Table 1 and correlate with the electron-donating or –releasing nature of the diimine substituents. The generation of this compound probably takes place via the reactions described in equations 3 and 4; here a disproportionation reaction of $\mathbf{1}^{+}$ initially yields $\mathbf{1}^{2+}$, a sixteen-electron octahedral species that associates with a weak donor species, probably PF_6^- from the electrolyte. Seven-coordinate tungsten(II) carbonyl compounds such as these are well established,[18] and their generation via electrochemical processes has previously been reported.[19] In addition, the above reaction pathway is consistent with the well-established tendency of d^5 carbonyl species to undergo disproportionation reactions, especially when stabilization via isomerization is not possible.[20]

$$2\,[W(CO)_4(LL)]^{+} \rightleftharpoons W(CO)_4(LL) + [W(CO)_4(LL)]^{2+} \quad (3)$$

$$[W(CO)_4(LL)]^{2+} + D \longrightarrow [W(CO)_4(LL)(D)]^{2+} \quad (4)$$

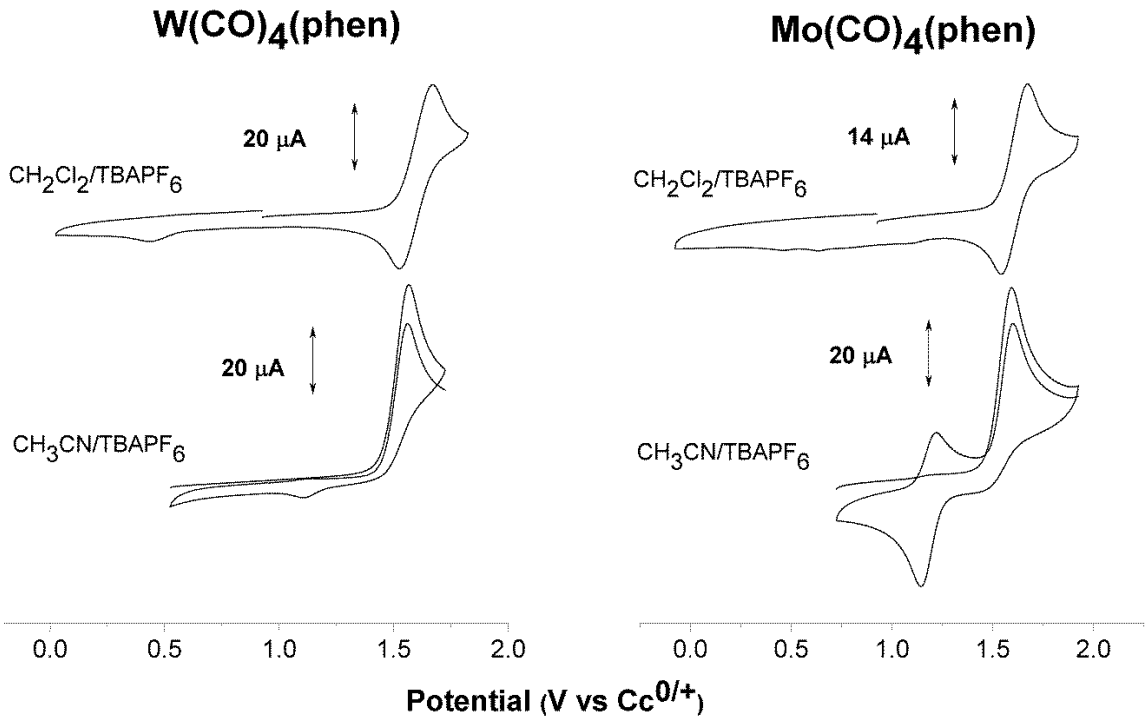

Figure 1. Cyclic voltammograms of **1a**, left, and $Mo(CO)_4(phen)$, right in $CH_2Cl_2/TBAPF_6$, top row, and $CH_3CN/TBAPF_6$, bottom row, obtained at a 3mm diameter glassy carbon electrode at scan rates of 0.25 V s^{-1}; concentrations in each case are 2.0 mM, except for that shown in the top right panel, for which the analyte concentration was 1.4 mM.

Consistent with the above proposed reaction scheme is the fact that cyclic voltammograms of **1** show a second oxidation that is broad and irreversible. The species formed by second process, presumably $\mathbf{1}^{2+}$, would be expected to be very electron deficient, and therefore highly Lewis acidic, making its subsequent association with an electron donor, even a weak one such as PF_6^-, to be quite favorable. Notably, the current of the coupled reduction peak at about 0.3 V vs $Cc^{0/+}$ is markedly enhanced when the initial anodic sweep extends to the second irreversible oxidation peak described above (Figure 2a); $[W(CO)_4(LL)D]^{2+}$ can, therefore, be generated via chemical and electrochemical routes.

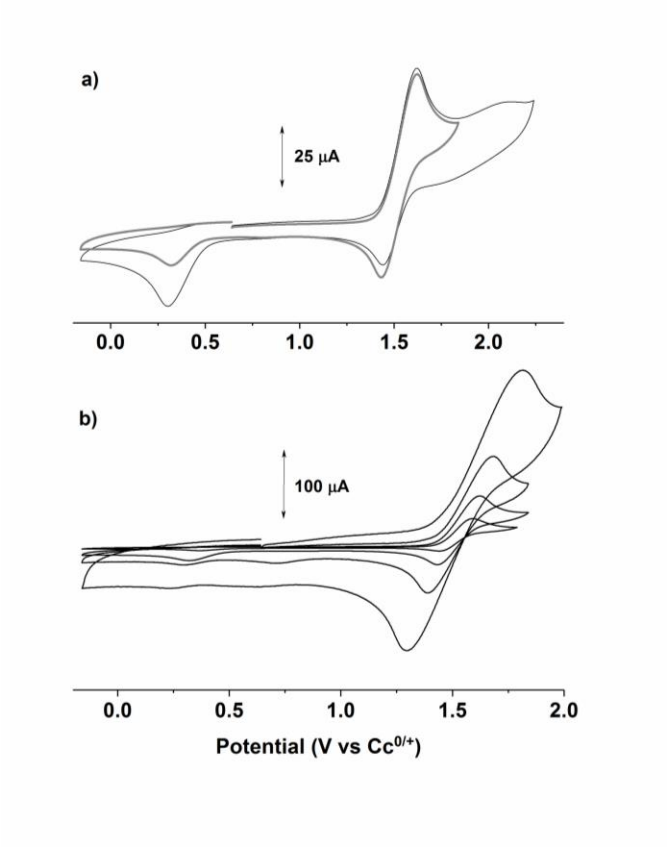

Figure 2: a) Cyclic voltammograms of 2.1 mM **1a** obtained at 0.25 V s^{-1}; when the anodic sweep extends beyond the first oxidation process (thin black line) there is substantial current enhancement for the peak we assign to the tungsten (II) disproportionation product, at 0.32 V, then when the switching potential is between the two anodic processes (thick gray line); b) a scan rate study of 2.1 mM **1a**; scan rates employed were 0.05, 0.25, 1.0, and 5.0 V s^{-1}; the presence of two small reduction processes, at 0.32 and 0.73 V, are discernable at 1.0 and 5.0 V s^{-1}. The increased peak separation for the $\mathbf{1a}^{0/+}$ couple observed at higher scan rates is due to uncompensated resistance in the electrochemical cell.

Additional evidence that supports the above reaction scheme includes the following. Spectroelectrochemical experiments (see below) indicate that $[W(CO)_4(ncp)]^+$, **1f⁺**, decomposes to form the parent compound, **1f**, and a tungsten carbonyl species with an oxidation state greater than +1, presumably due to disproportionation. We also collected kinetic data (see below) show that most **1⁺** compounds reacts via a reaction that is second-order with respect to the radical cation. Finally, it is worth noting that voltammograms of the structurally similar *cis*-$W(CO)_4(\eta^2$-olefin) compounds measured in weakly coordinating media bear are striking resemblance to that shown in Figure 1 and may be indicative that similar homogeneous coupled chemistry is operative in those systems.[21]

While the simplicity of the voltammogram of **1a** in CH_2Cl_2/$TBAPF_6$ may suggest that disproportionation is the sole reaction that **1⁺** radicals undergo in weakly coordinating media, scan rate studies of **1** indicate that **1⁺** also undergoes a parallel reaction pathway (Figure 2b). The voltammograms of **1a** obtained at 1.00 V s^{-1} features two small coupled reduction peaks in addition to those of the $\mathbf{1a}^{0/+}$ couple. That at the more negative potential is assigned to the disproportionation product, $[W(CO)_4(phen)D]^{2+}$. Based on similarities to the molybdenum analogs, we assign the peak at the greater potential to the reduction of $[W(CO)_3(LL)D]^+$, formed via loss of a carbonyl ligand and association with a donor species, D. The precise nature of D is not clear, as both PF_6^- and H_2O could plausibly complete the octahedral coordination sphere of the tungsten(I) metal center. The fact that this peak is not seen at lower scan rates indicates that these tricarbonyl species are relatively short-lived; it is likely that if D is a poor ligand, decomposition by additional loss of carbonyl ligands would result owing to the electron-deficient nature of the metal center. It is notable that at higher scan rates, these two coupled reduction peaks have similar currents, suggesting that the processes that give rise to those signals occur at similar rates under the conditions employed. This is consistent with chronocoulometric data, described below, that indicate **1⁺** species react via parallel pathways, one of which is first-order, and the other second-, with respect to the radical cations.

More dramatic differences between the voltammograms of the molybdenum and tungsten compounds were observed in CH_3CN/$TBAPF_6$. (Figure 1, bottom) While the irreversibility of the bulk oxidation processes of these $M(CO)_4(LL)$ complexes indicate that both the tungsten(I) and molybdenum(I) radicals are rapidly attacked by solvent molecules,[22] only the molybdenum compound shows a large reversible couple, assigned to $[Mo(CO)_3(LL)(CH_3CN)]^+$; the corresponding peak assignable to $[W(CO)_3(LL)(CH_3CN)]^+$ is detectable but has a much smaller

current. We later describe additional experiments that further shed light on this coupled chemistry.

Kinetic Studies of $[W(CO)_4(LL)]^+$ Disproportionation. To get further insight into the chemical reactions coupled to the oxidation of **1**, we performed a series of kinetic studies using double potential-step chronocouometry. In these experiments, we measured the charge passed in a timed step over the bulk oxidation process and then in a reverse step involving only reduction of the electrogenerated species; potentials were chosen such that no other coupled reductions would be effected during the reverse step. Plots of the charge ratio, Q_f/Q_r, against either log $k\tau$ or log k[**1**] τ, where k is the rate constant for the operative reaction and τ is the step time of the experiment, were compared against working curves of several likely mechanisms, including those for a simple first order pathway and a second-order disproportionation.[15]

Data obtained for several concentrations of **1a** are presented in Figure 3 along with the theoretical response for a disproportionation reaction. For a given step time, the charge ratios observed were clearly affected by the concentration of the bulk species, suggesting that the coupled homogeneous chemistry is second order with respect to the cation radicals. Indeed, experimental data obtained at every given concentration of analyte fit the working curve for a disproportionation very well. However, the best fit rate constants for each such set of measurements showed a systematic variation, with the best fit rate constants apparently decreasing with increasing tungsten concentration. This is consistent with a scenario involving simultaneous reactions: a disproportionation and separate first order reaction involving $\mathbf{1a}^+$. The rate constants employed in the x axis of the graph shown in Figure 2, consequently, represent effective overall rate constants, k_{eff}, that have contributions from two distinct pathways and which have different values for each concentration examined. Using the approach described in the Experimental Section, we estimate that rate constants for the disproportionation, k_{disp}, and the first order process, $k_{1storder}$, to be 400 M^{-1} s^{-1} and 0.3 s^{-1}, respectively. Thus at the concentrations employed for these studies, 0.5 to 2.5 mM, these are competitive processes, as indicated by the voltammetric scan rate study described above. We suspect that decarbonylation/substitution is the major first order event, as described above.

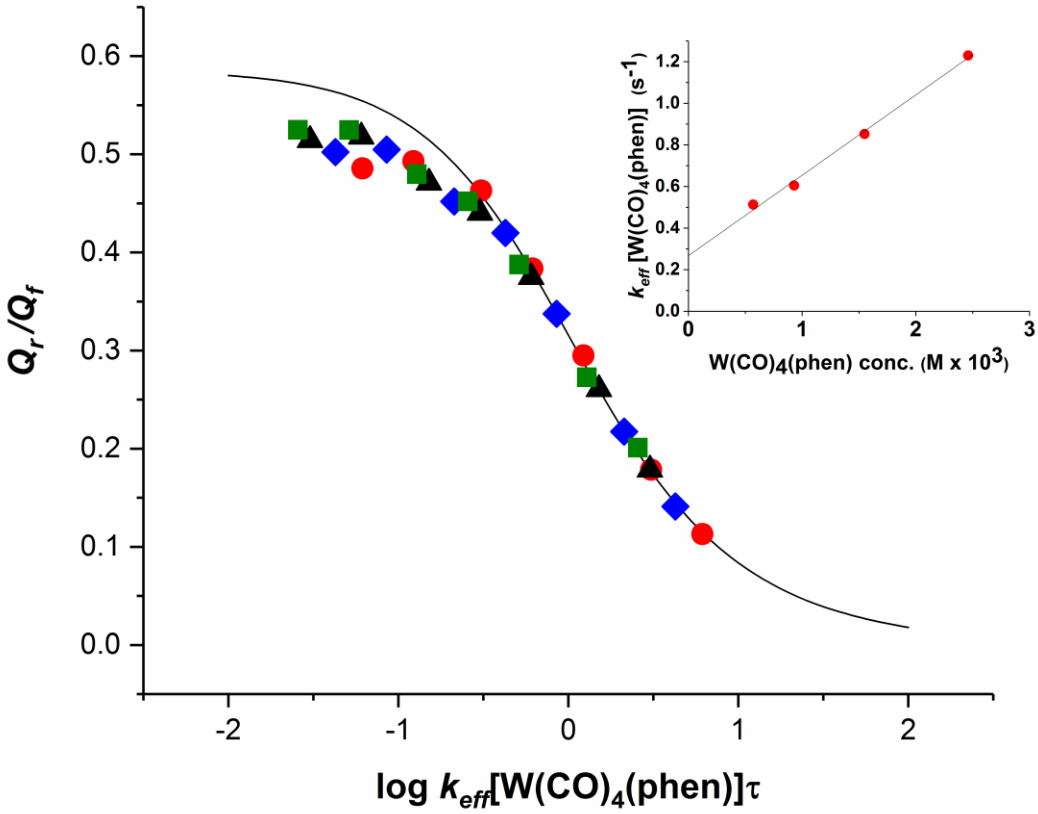

Figure 3. Double potential-step chronocoulometry results obtained for 0.6 (■), 0.9 (▲), 1.6 (◆) and 2.5 (●) mM **1a** in CH_2Cl_2/$TBAPF_6$. Step times, τ, ranged from 0.05 to 5 s. The potential step was 0.5 V and was centered on the bulk oxidation peak of the corresponding cyclic voltammogram. Each concentration was individually fit to the theoretical working curve (solid line) of a disproportionation reaction of the **1a**$^+$. Best fit rate constants, k_{eff}, were 900, 650, 550 and 500 M^{-1} s^{-1} for the four concentrations examined, from lowest to highest. Inset: k_{eff}[**1a**] values as function of the bulk **1a** concentration; the slope and intercept of this plot yields estimates of k_{disp} and $k_{1st\text{-}order}$, respectively. From these data the following rate constants were calculated: k_{disp} = 400 M^{-1} s^{-1} and $k_{1st\text{-}order}$ = 0.3 s^{-1}.

Results similar to those above were obtained for most of the other compounds so analyzed; k_{disp} values are presented in Table 1. Of particular note is the observation electron-donating substituents on the diimine ligands increase the values of k_{disp}; for example, the disproportionation rate constant of [W(CO)$_4$(dmb)]$^+$, **1j**$^+$, is greater than that of the bpy analog, **1b**$^+$, by roughly a factor of three. We speculate that this is a result of a stabilization of the resulting tungsten(II) disproportionation product by the increased electron donation from the diimine ligand.

An important exception to the reactivity described above was observed for $[W(CO)_4(ncp)]^+$, **1f**$^+$, which appears to decay via a simple first order process with $k_{1st\text{-}order}$ = 0.07 s^{-1}. This is consistent with the lack of an obvious peak on the cyclic voltammogram ascribable to the corresponding disproportonation product (Figure 4, inset). The methyl substituents of the ncp ligand are adjacent to the nitrogen donor atoms and thereby serve to sterically block the metal center. This bestows kinetic stability on otherwise reactive species by reducing access to the metal center by potential nucleophiles.[8, 23] Similarly, the rate of disproportionation of $[W(CO)_4(bcp)]^+$, **1g**$^+$, which is also sterically crowded, is less than that of its unmethylated analog $[W(CO)4(bph)]^+$, **1e**$^+$.

Interestingly, infrared spectroelectrochemical experiments (see below) strongly suggest that **1f**$^+$ does, in fact, disproportionate. We attribute this to a ligand-induced pathway, in which association with a donor species is the rate determining step in the mechanism, giving rise to the observed first order kinetics; this is discussed in greater detail in the following section. Finally, the significantly greater rate of disproportionation of **1g**$^+$ compared to **1f**$^+$ is curious. They both are sterically hinder by methyl groups in the 2- and 9- positions of the phenanthroline ligand so would be expected to show similar steric effects. An alternate pathway for electron transfer may therefore exist that involves the phenyl substituents rather than direct or bridged interaction between the metal centers.

Infrared Spectroelectrochemistry of W(CO)4(ncp), 1f, and W(CO)4(bcp), 1g. The kinetic stability afforded by the methyl groups of ncp and bcp described above, raised to us the possibility that the corresponding **1**$^+$ radical cations, **1f**$^+$ and **1g**$^+$, may be long-lived enough to characterize by room-temperature infrared spectroelectrochemistry. Infrared spectra collected during a bulk electrolysis of **1f** in a flow-through cell equipped with a gold-mesh working electrode are presented in Figure 4a. The observed shift to higher frequencies of the carbonyl stretches as well as the decrease in absorption intensities are consistent with an oxidation that is primarily tungsten-centered.[8,11,21] The fact that four discernible stretches are observed in the carbonyl region, peaks at 2085, 1990, 1960 and a shoulder at 1938 cm^{-1}, is notable as this shows that none of the carbonyl ligands are lost by **1f**$^+$ under these conditions. We also note the pattern of carbonyl peaks, in terms of their relative intensities, is distorted upon oxidation and may be indicative of a structural perturbation induced by ion pairing with the supporting electrolyte. Bulk oxidation of **1g** yielded very similar spectra (Figure SI-1), showing new peaks at 2084, 1989, 1956 and 1940 cm^{-1}. These are, to our knowledge the examples of spectroscopic characterization of tungsten tetracarbonyl radical cations of diimine ligands.

Useful comparisons can be made between the infrared spectra presented above and those of related compounds. While the spectra of $[Cr(CO)_4(tmp)]^+$ and $[Mo(CO)_4(ncp)]^+$ are very similar to each other,[6,8] they differ somewhat from the tungsten(I) species in this work. Most significantly, while the carbonyl peaks for the parent $M(CO)_4(LL)$ compounds for all three Group 6 metals are very similar, those for **1f**$^+$ and **1g**$^+$ are substantially lower than those for the isoelectronic chromium and molybdenum species; the symmetric peak is about 10 cm^{-1} lower, while the asymmetric stretches are lower by an average of about 40 cm^{-1}. This could be indicative of a stronger interaction between the metal center and the PF_6^- supporting anion; such an interaction would be expected to be minimal in the chromium analog due to size constraints, but could be important for tungsten. The carbonyl stretching frequencies reported for *cis*-$[W(CO)_4(\eta^2\text{-}C_2H_4)]^+$ are considerably higher[21] than we see for **1f**$^+$ and **1g**$^+$ but this can be attributed to differences between the diimine and olefin ligands; the observed peak shifts between the neutral parents and radical cations are actually quite similar, averaging about 100 cm^{-1} in each case.

The spectra in Figure 4a show isosbestic behavior until about 70% of the electrolysis is complete, when second, more highly oxidized species, becomes evident. We attribute this to a tungsten disproportionation product. Evidence for this assignment comes from infrared spectra collected after nearly exhaustive oxidation of **1f**; after termination of the applied potential, peaks attributable to two products grew in intensity, nearly isosbestically, as those due to the radical cation decreased (Figure 4b). One set of product peaks was due to the parent compound, **1f**, while the other has carbonyl peaks at 2101, 2012, 1997, and 1925 cm^{-1}, higher than those assigned to **1f**$^+$ and consistent with a more highly oxidized metal tetracarbonyl.

To reconcile the spectral changes presented in Figure 4b with the chronocoulometric data described earlier, we propose that a ligand-induced disproportionation is operative with **1f**$^+$, as explained below. First, **1f**$^+$ undergoes a slow associative reaction with a donor species, D, such as PF_6^-, thereby converting the seventeen-electron electrogenerated species to a nineteen-electron species (eq. 5) capable of serving as a reducing agent. The subsequent electron transfer (eq. 6) then yields two eighteen-electron species. We have previously observed similar behavior by other electrogenerated species, including $[Mo(CO)_3(LL)(CH_3CN)]^+$ and $[CpFe(CO)_2]_2$.[8, 24]

$$[W(CO)_4(ncp)]^+ + D \rightleftharpoons [W(CO)_4(ncp)(D)]^+ \quad (5)$$

$$[W(CO)_4(ncp)]^+ + [W(CO)_4(ncp)(L)]^+ \longrightarrow W(CO)_4(ncp)(L) + [W(CO)_4(ncp)(L)]^{2+} \quad (6)$$

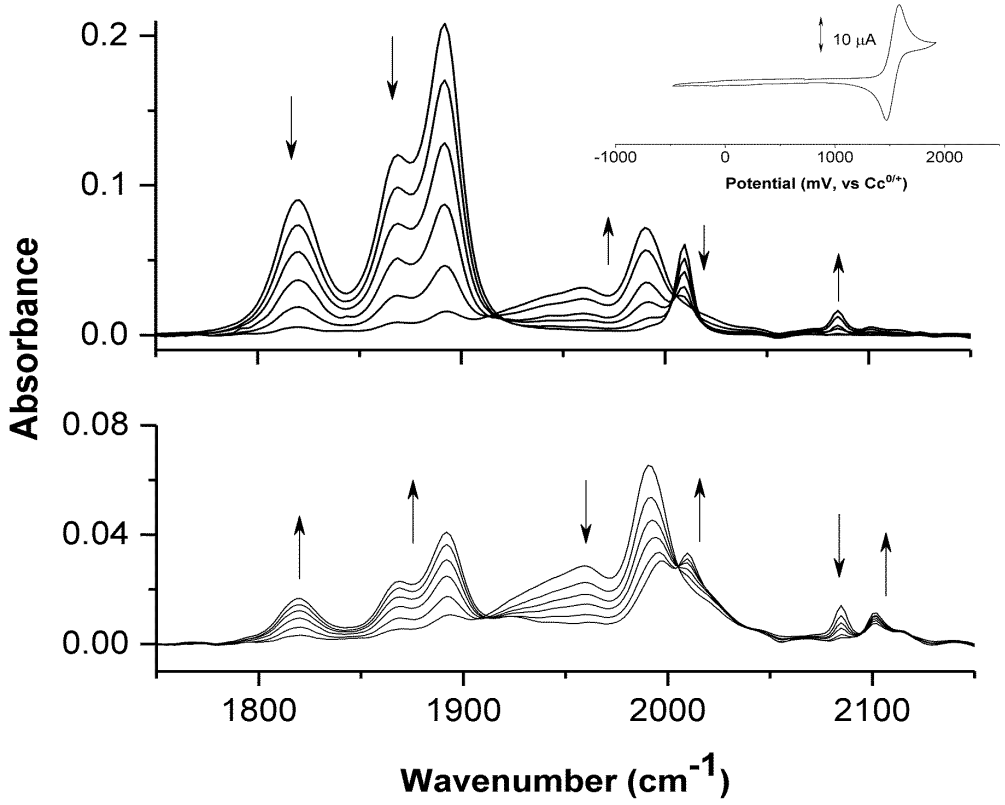

Figure 4: (*a*, top) Changes in infrared spectra of the carbonyl region during room temperature thin-layer bulk electrolysis of $W(CO)_4$(ncp), **1f**, at 0.2V positive of the $E_{1/2}$ value observed on the voltammogram (inset); (*b*, bottom) infrared changes observed upon reaction of the electrogenerated radical cation $\mathbf{1f}^+$ after termination of the electrolysis; total elapsed time for the reaction is about 3 minutes. Arrows indicate the direction of change for the peaks heights.

Large amplitude ac cyclic voltammetric studies. To get further insight into the heterogeneous electron-transfer processes associated with the oxidation of **1**, as well as the coupled homogeneous chemistry, we performed large amplitude ac voltammetry on **1a**. The third through sixth harmonics obtained for 0.3 mM **1a** are shown in Figure 5. These data are consistent with a fast heterogeneous electron transfer; simulations suggest that the standard rate constant for the electron transfer has a lower limit of about 0.2 cm s^{-1}, similar to that we observed for ferrocene under similar conditions.[25]

A comparison of our chronocoulometric observations for **1a** with the ac voltammetry results was particularly illuminating. We initially attempted to fit the data in Figure 5 with a scheme identical

to that suggested by the chronocoulometric data discussed above, that is, to an irreversible disproportionation mechanism taking place alongside a parallel first-order decay. Interestingly, this model did not yield satisfactory agreement with experimental data (Figure SI-2); specifically, the ratio of peak heights within the envelopes for the forward and reverse sweeps could not be satisfactorily simulated (Figure SI-2). Good agreement was achieved, however, by employing a scheme in which the disproportion was rapidly reversible, as defined in eq. 3, above; our previous study using this technique demonstrated that the response of ac voltammetry is highly sensitive to the existence of equilibria involving electrogenerated species.[26] The fits shown in Figure 5 were generated using a mechanistic scheme that included a first-order follow-up reaction, with rate constant k_2, involving the tungsten (II) disproportionation product (eq. 4) that gives rise to the species responsible for the coupled reduction peak seen on the dc voltammograms, as well as a first order decay process for **1a**$^+$ with rate constant k_3. Based on the peak shapes, we estimate that rate constants of the disproportionation equilibrium, k_1 and k_{-1}, are 2×10^4 M^{-1} s^{-1} and 1×10^5 M^{-1} s^{-1}, respectively. Thus, the thermodynamic driving force for the disproportionation, it seems, is fairly modest.

Reactivity of $[W(CO)_4(LL)]^+$ Toward Lewis Bases.

As exemplified by the voltammograms in Figure 1, the homogeneous coupled chemistry followed by **1** and its molybdenum analogs differ substantially in coordinating media. It is likely that these divergent behaviors have a kinetic basis, that is, while the essential reaction schemes followed by these species are probably similar, the relative rates of the competing reactions are not, manifesting their distinctive electrochemical responses. To get further insight into the competing reactions followed by **1**$^+$, we undertook a number of studies that examined the reactivity of electrogenerated **1a**$^+$ and **1b**$^+$ in the presence of varying levels of two added ligands, pyridine and acetonitrile.

Voltammograms of **1b** obtained in the presence of pyridine (pK_b = 9, 1.6 equivalents) and acetonitrile (pK_b = 25, 1.6 equivalents) are presented in Figure 6 (bottom and middle traces, respectively). These results show that the rate of attack by the base on **1**$^+$, as well as the relative conversion of **1**$^+$ to the corresponding substitution product, $[W(CO)_3(LL)(LB)]^+$, where LB is the substituting Lewis base, both increase with base strength. With respect to the first point, the reversibility of the bulk oxidation process for **1b** is essentially lost in the presence of even subequivalent levels of pyridine (Figure SI-3), whereas a detectable return peak due to the

reduction of **1b**$^{+}$ is discernable at up to 3.2 equivalents acetonitrile (data not shown).With respect to the second point, the response of **1b** in the presence of 1.6 equivalents of acetonitrile is intriguing because, while it is clear that the presence of acetonitrile greatly diminishes the lifetime of the radical cation, there is virtually no acetonitrile substitution product observed under the otherwise identical reaction conditions. This is not due to any inherent instability of this species as related experiments in our lab show that the oxidation of $W(CO)_3(LL)(CH_3N)$ is chemically reversible under similar conditions.

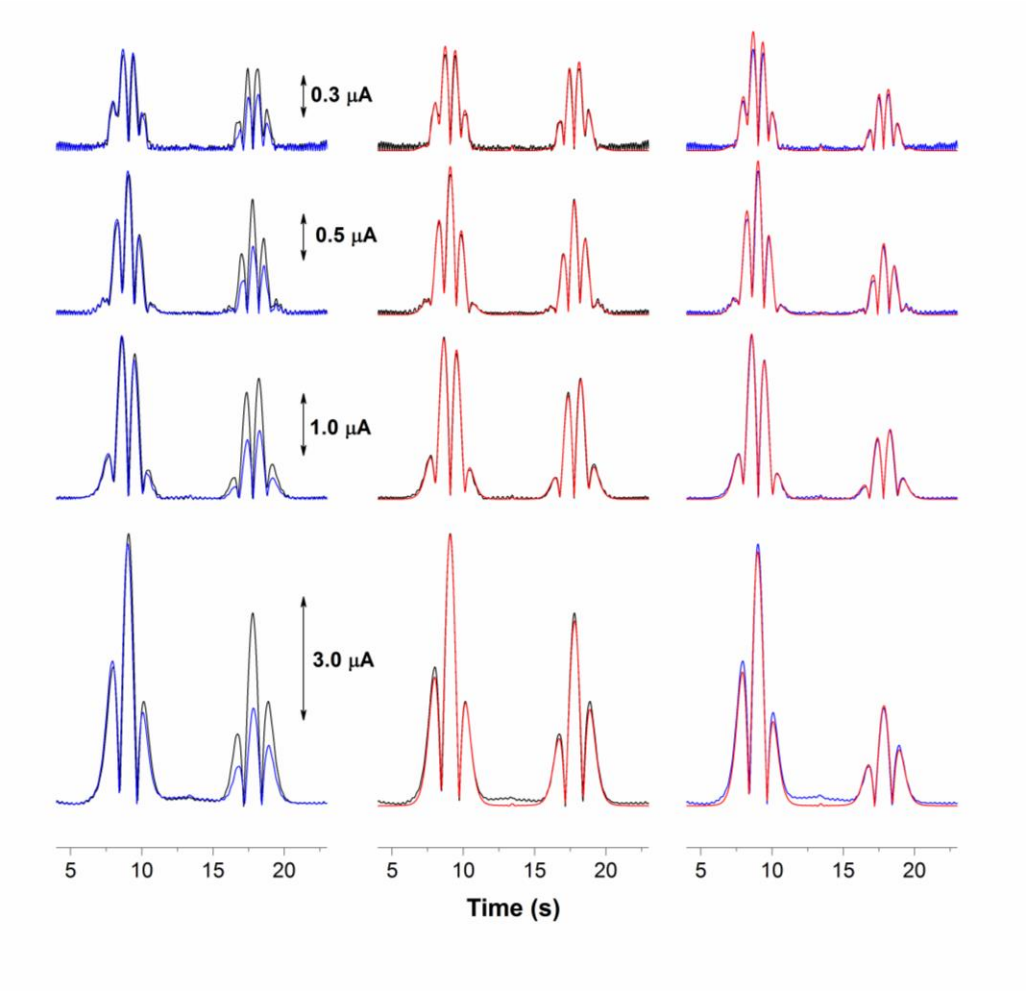

Figure 5. Third (bottom row) through sixth (top row) harmonics of large amplitude ac voltammetry results of 0.28 mM **1a** in the presence of no added acetonitrile (black traces) and 3.2 mM acetonitrile (blue traces); red traces show optimized fits for the two sets of data. The switching time in each experiment was 13.4 s; peaks observed at earlier times correspond to those occurring during the anodic sweep, those at longer time are from the cathodic sweep. Experimental parameters are: scan rate = 0.0894 V s^{-1}, electrode area = 0.071 cm^2, ac amplitude, ΔE = 0.1 V, frequency = 13.49 Hz. Simulation parameters that were kept constant in the two simulations were the diffusion coefficient = 1.2×10^{-5} cm^2 s^{-1}, $k°$ = 0.30 cm s^{-1}, and the homogeneous rate constants (see Scheme 1) $k_1 = 2 \times 10^4$ M^{-1} s^{-1}, $k_{-1} = 1 \times 10^5$ M^{-1} s^{-1}, k_2 = 0.35 s^{-1}, k_3 = 500 M^{-1} s^{-1} , k_{-3} = 40 s^{-1}, and $k_4 = 1 \times 10^6$ M^{-1} s^{-1} ; uncompensated resistance varied slightly in the two simulations (250 Ω and 220 Ω, in the absence and presence of acetontrile, respectively).

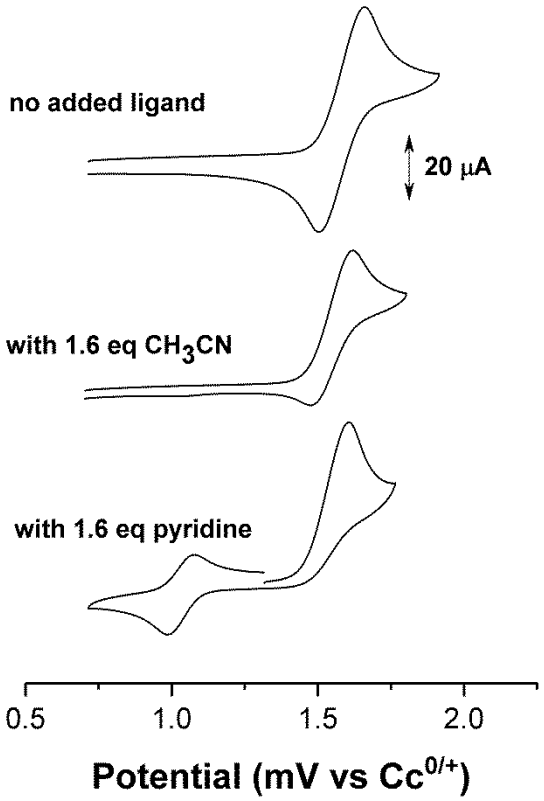

Figure 6: Cyclic voltammograms of 2.0 mM **1b** in CH_2Cl_2/$TBAPF_6$ with (top) no added ligand, (middle) 1.6 equivalents of acetontrile, and (bottom) 1.6 equivalents of pyridine; scan rates in each case are 0.25 V sec^{-1}.

The extent of the substitution reaction in each case is more fully illustrated by a plot of the peak current ratios, $i_{c,sub}/i_{a^\circ}$ as a function of added ligand concentration, where $i_{c,sub}$ is the peak current of the substitution product reduction and i_{a° is that of the bulk oxidation in the absence of added ligand (Figure SI-4). To summarize, the substitution product grows in much more quickly in the case of pyridine and reaches a limiting concentration that is significantly than is seen with acetonitrile.

A reaction sequence that accounts for these observations is presented in Scheme 1 and described briefly below. The substitution reaction that gives rise to the reversible couple at about 1.1 V is summarized by equation 7 and likely proceeds via an associative mechanism because the carbonyl ligand is not labilized to this extent upon oxidation of **1** in the absence of added ligands. Presumably, attack by the Lewis base results in a nineteen-electron, seven-coordinate species (eq 8), which is then followed by loss of one CO ligand. The associative

nature of the reaction has many precedents with other 17-electron species[27] and is supported by double potential-step chronocoulometry studies of **1a** and **1b** (data not shown) that indicate the reaction between $\mathbf{1}^+$ and added base is first-order in both species.

$$[W(CO)_4(LL)]^+ + LB \longrightarrow [W(CO)_3(LL)(LB)]^+ + CO \quad (7)$$

$$[W(CO)_4(LL)]^+ + LB \rightleftharpoons [W(CO)_4(LL)(LB)]^+ \quad (8)$$

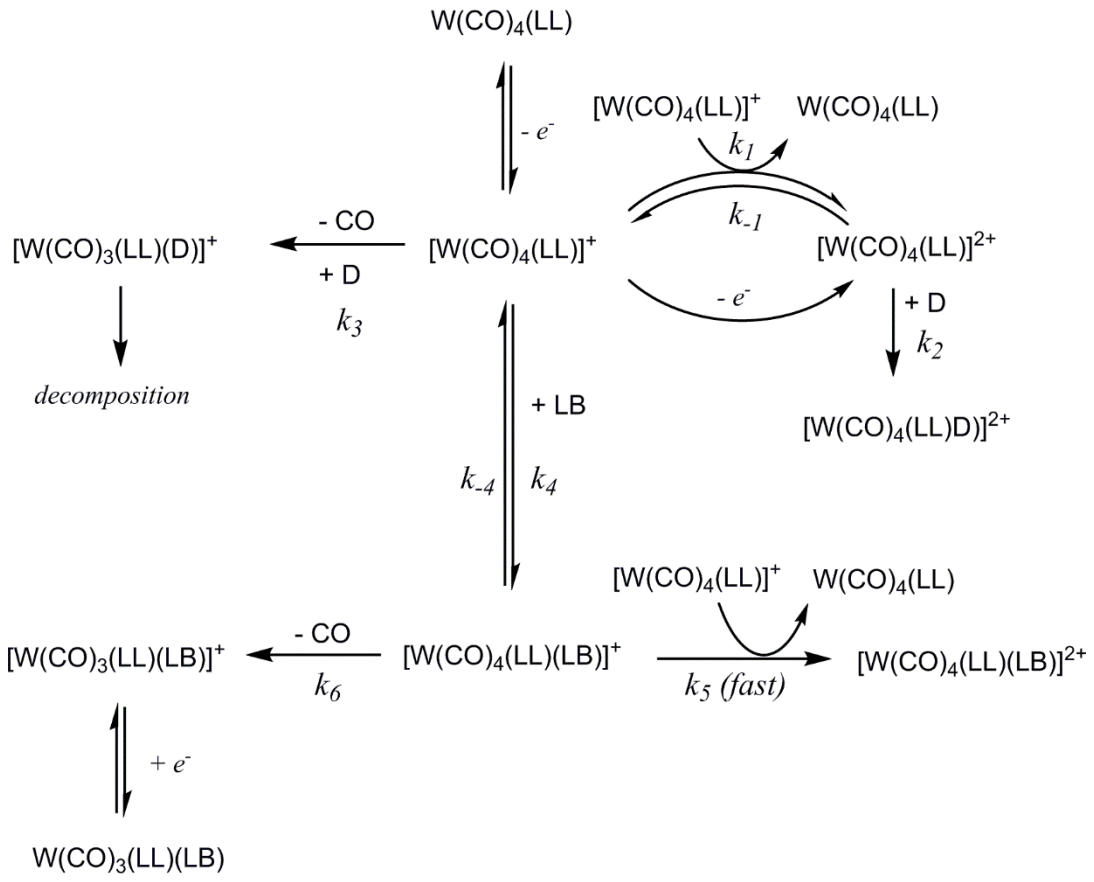

Scheme 1. Summary of observed chemistry followed by electrogenerated $\mathbf{1}^+$ species; rate constants are discussed in the text; LB is an intentionally added Lewis base that can serve as a ligand (pyridine or acetonitrile in this work) and D is a coordinating species in the solvent electrolyte such as PF_6^- or adventitious water.

The initial slopes of the $i_{c,sub}/i_{a^\circ}$ plot shown in Figure SI-4, which reflects the rate of the substitution process at low concentrations of added ligand, provides insight into the rate constants of the reaction shown by equation 8 (k_4 in Scheme 1); based on these data, k_4 is

substantially greater for pyridine than for acetonitrile, consistent with the higher basicity of the latter. Also of interest are the apparent limiting values of $i_{c,sub}/i_{a^\circ}$, which are about 0.40 and 0.15 for pyridine and acetonitrile, respectively; for comparison, simulations indicate that in the absence of any competing reactions, the limiting value, that is the value of $i_{c,sub}/i_{a^\circ}$ that would be observed if 100% of electrogenerated **1**$^+$ is converted to the corresponding substitution products, would be 0.64. Thus about two-thirds of **1b**$^+$ undergoes net substitution in the presence of pyridine, while only about one-quarter does so in the presence of acetonitrile. This clearly reflects a competition between reaction pathways that is affected by base strength.

We propose that the major reaction that competes with CO substitution is a ligand-induced disproportionation, analogous to that described previously for the reaction of **1f**$^+$ observed via infrared spectroelectrochemistry. Specifically, the 19-electron intermediate shown in equation 8 can serve as a reducing agent toward **1**$^+$(eq 9). The rate of such a reaction would be maximized when the concentrations of the 17- and 19-electron reactants are the same. The competition with the substitution pathway, therefore, will be greatest when either the base employed has an equilibrium constant, K_4, that is not so large that it saturates **1**$^+$, or when the concentration of base is such that that enough **1**$^+$ is present to react with the 19-electron ligand adduct. The relative portion of substitution products will be affected by base in two ways. First, increasing base strength will increase K_4, and therefore suppress disproportionation at relatively high base concentrations, giving rise to the saturation kinetics seen in Figure SI-4. Second, the rate of CO loss (rate constant k_5 in Scheme 1) by the 19-electron ligand-adduct could also be influenced by structural and electronic factors of the substituting ligand. The data shown in Figure SI-4 would indicate that pyridine has a larger equilibrium constant, K_4, relative to acetonitrile, consistent with its greater basicity, and suggests that the rate of decarbonylation for the 19-electron adduct is also greater with pyridine, perhaps due to greater stabilization of the transition state associated with the loss of CO from the tungsten (I) center.

$$[W(CO)_4(LL)(LB)]^+ + [W(CO)_4(LL)]^+ \longrightarrow [W(CO)_4(LL)(LB)]^{2+} + W(CO)_4(LL) \quad (9)$$

As we indicated above, large-amplitude ac voltammetry is sensitive to the presence of equilibria involving electroactive species, so is ideal for examining the reaction between **1**$^+$ and added ligands. We therefore used this technique to examine the reaction of **1a**$^+$ toward acetonitrile (Figure 5, blue traces). Most notable about the results compared to those obtained in the absence of added ligand is the decrease in peak currents in the return sweep. Our data fit simulations (Figure 5, red traces) of a mechanism involving a rapid equilibrium between **1a**$^+$ and

the corresponding 19-electron acetonitrile adduct; the lower limit of the forward rate constant appears to be roughly 100 M^{-1} s^{-1} and the equilibrium constant for the reaction is estimated to be approximately 1×10^5.

The reaction pathways outlined in Scheme 1 are supported by several additional observations worth noting. For example, additional dc cyclic voltammetry experiments show that as acetonitrile is added to solutions of **1a** and **1b**, there is a significant increase current of the reduction peak assigned to the tungsten(II) disproportionation product, as well as a shift in the peak potential; this supports our contention that the rate of disproportionation is indeed enhanced by the presence of coordinating ligands. In addition, Scheme 1 predicts current enhancement of the bulk oxidation peak, due to the regeneration of the parent compound, **1**, via the disproportionation step especially in concentration regimes lower than those showing saturation behavior, this was especially notable in the titration with pyridine at levels between about 3 and 25 equivalents of ligand. At higher concentrations of ligand, this current enhancement faded, presumably because the equilibrium is shifted so strongly in favor of the pyridine adduct, that the concentration of 1b+ is small enough to make the disproportionation a minor reaction compared to ligand substitution.

Finally, we should note that the coupled chemistry associated with oxidation of **1** in the presence of added ligands is almost certainly more complex than indicated by Scheme 1. The substitution products, for example, are themselves electroactive at the potentials employed in this study and undergo disproportionation reactions; they will likely react with some of the species we directly observed in this work. In addition, the work of Hanzlik et al. with $Mo(CO)_4(bpy)$ showed “curve-crossing” under some conditions that they attributed to oxidation of the parent compound by molybdenum (II) species generated via disproportionation.[8] We observed similar behavior in these studies under some conditions, indicating that the tungsten (II) products we invoke in the above discussions are not innocent and will likely introduce additional reactions not included in Scheme 1.

Summary of $[M(CO)4(LL)]^+$ Reactivity

Despite the substantially different cyclic voltammograms exhibited by **1a** and its molybdenum analog in $CH_3CN/TBAF_6$, the chemistry of respective electrogenerated cations appear to share the same reaction pathways, albeit with significant differences in their relative reaction rates. The general reaction pathways are summarized in Scheme 1 and briefly summarized below.

The radical cations, $\mathbf{1}^{+}$, are generated via a fast electrode process; ac voltammetry studies indicate that the radicals exist in equilibrium with unassociated disproportionation products **1** and $\mathbf{1}^{2+}$. In weakly coordinating media, $\mathbf{1}^{2+}$ associates with donor species, D, which could be supporting anions or adventitious water, yielding $[W(CO)_4(LL)(D)]^{2+}$ which is readily seen on cyclic voltammograms. $\mathbf{1}^{+}$ can also lose a carbon monoxide ligand, giving relatively short-lived species $[W(CO)_3(LL)(D)]^{+}$, observable on cyclic voltammograms obtained using scan rates of about 1 V s^{-1} or greater.

In the presence of Lewis bases, such as nitrogen donor species, $\mathbf{1}^{+}$ expands its coordination sphere, yielding the nineteen-electron species $[W(CO)_4(LL)(LB)]^{+}$; this can reduce $\mathbf{1}^{+}$ or lose a carbonyl ligand to generate the substitution product $[W(CO)_3(LL)(LB)]^{+}$. The latter pathway is favored by **1** at low concentrations of added ligand or in the presence of high concentrations of weak nitrogen donors such as acetonitrile. In contrast, ligand substitution is favored by stronger donors such as pyridine, and appears to be the path followed by molybdenum even in the presence of weak bases such as acetonitrile. Current work in our lab is focused on investigating additional aspects of the coupled chemistry described above, especially at low levels of added base.

References.

[1] A. Vlček, Jr. *Coord. Chem. Rev*. **2002**, 230,225.

[2] a) M. L. Clark, K. A. Grice, C. E. Moore, C. P. Kubiak, *Chem. Sci.*, **2014**, *5*, 1894; b) J. Tory, B. Setterfield-Price, R. A. W. Dryfe, F. Hartl, *ChemElectroChem*., **2015**, *2*, 213.

[3] A. A. Vlček, *Chemtracts – Inorg. Chem*, **1993**, *5*, 1.

[4] S. Ernst, W. Kaim, *J. Am. Chem. Soc.* **1986**, *108*, 3578.

[5] E. Ioachim, G. S. Hanan, *Can. J. Chem.* **2005**, *83*, 1114.

[6] Farrell, I. R.; Hartl, F.; Záliš, S.; Wanner, M.; Kaim, W.; Vlček Jr., A. *Inorg. Chim. Acta,* **2001**, *318*, 143.

[7] Hanzlík, J.; Pospíšil, L.; Vlček, A. A.; Krejčík, M. *J. Electroanal Chem*. **1992**, *331*, 831.

[8] R. Johnson, H. Madhani, J. P. Bullock, *Inorg. Chim. Acta* **2007**, *360*, 3414.

[9] W. Kaim, S. Kohlmann, *Inorg. Chem*. **1987**, *26*, 68.

[10] W. Strohmeier*, Angew. Chem., Int. Ed. Engl*. **1964**, *3*, 730.

[11] J. P. Bullock, D. C. Boyd, K. R. Mann, *Inorg. Chem.* **1987**, *26*, 3084.

[12] A. M. Bond, N. W. Duffy, S.-X. Guo, J. Zhang, D. Elton, *Anal. Chem.* **2005**, *77*, 186A.

[13] A. J. Bard, L. R. Faulkner, *Electrochemical Methods: Fundamentals and Applications, 2nd ed.;* Wiley: New York, 2001, Chapter 5

[14] G. F. Kennedy, A. M. Bond, A. N. Simonov, *Curr. Opin. in Electrochem*. **2017**, *1*, 140.

[15] Tom Dieck, H.; Kühl, E. *Z. Naturforsch. B: Anorg. Chem., Org. Chem.* **1982**, *37B*, 324.

[16] Hill, M. G.; Lamanna, W. M.; Mann, K. R. *Inorg. Chem.* **1991***, 30,* 4687–4690.

[17] R. Colton, *Coord. Chem. Rev.* **1971**, *6*, 269.

[18] A. M. Bond, R. Colton, K. McGregor, *Organometallics*. 1**990**, *9*, 1227.

[19] Bond, A. M., Colton, R. *Coord. Chem. Rev.* **1997**, *166*, 161

[20] J. Handzlik, F. Hartl, T. Szymańska-Buzar, *New J. Chem*. **2002**, *26*, 145.

[21] M. C. Baird, *Chem. Rev.* **1988***, 88,* 1217.

[22] Hanafey, M. K.; Scott, R. L.; Ridgway, T.H.; Reilley*, Anal. Chem.* **1978**, *50*, 116.

[23] J. P. Bullock, E. Carter, R. Johnson, A. T. Kennedy, S. E. Key, B. J. Kraft, D. Saxon, P. Underwood, *Inorg. Chem*. **2008**, *47*, 7880.

[24] J. P. Bullock, M. C. Palazotto, K. R. Mann, *Inorg. Chem*. **1991**, *30*, 1284.

[25] J. P. Bullock, E. Mashkina, A. M. Bond, *J. Phys Chem. A* **2011**, *115*, 6493.

[26] C.-Y. Lee, J. P. Bullock, G. F. Kennedy, A. M. Bond, *J. Phys. Chem A* **2010**, *114*, 10122.

[27] D. R. Tyler, *Prog. Inorg. Chem.* **1988**, *36*, 125.

Table 1. Summary of Electrochemical Characterization of $W(CO)_4(LL)$, 1, Compounds[A]

LL	$W(CO)_4(LL)$ letter designation	$E°$ (V vs $Cc^{+/0}$)	i_c/i_a	E_p [B] (V vs $Cc^{+/0}$)	k_{disp} [C] (M^{-1} s^{-1})
phen	**1a**	1558	0.65	0.349	400
bpy	**1b**	1564	0.78	0.386	240
dmp	**1c**	1522	0.58	0.307	*D*
tmp	**1d**	1500	0.66	0.360	780
bph	**1e**	1565	0.73	0.319	710
ncp	**1f**	1528	0.92	-0.015	*E*
bcp	**1g**	1544	0.85	-0.057	120
nop	**1h**	1629	0.65	0.487	*D*
clp	**1i**	1591	0.74	0.445	*D*
dmb	**1j**	1514	0.66	0.293	790

[A] Cyclic voltammograms obtained using CH_2Cl_2/$TBAPF_6$ at scan rates of 0.25 V s^{-1}; analyte concentrations were 1.0 ± 0.1 mM.

[B] Cathodic peak maximum assigned to the disproportionation product of $\mathbf{1}^+$.

[C] Rate constant for the disproportionation of $\mathbf{1}^+$ as determined by double potential-step chronocoulometry.

[D] Not measured.

[E] Chronocoulometric data did not satisfactorily fit the theoretical response for a disproportionation mechanism.